

It is well known^{5,6} that virtually all synthetic ZnS crystals contain appreciable numbers of stacking faults in the direction of the *c*-axis. These result in streaking between certain spots in the x-ray diffraction patterns obtained by precession about the *c*-axis. In some crystals, the faulting has sufficient periodicity so that "polytype" spots are also obtained. The crystals used in the present work exhibit primarily 3-layer stacking (cubic structure) with various amounts of random stacking reversals. Two crystals, No. 4 and 5, showed a small amount of the 2-layer (hexagonal) modification.

A natural supposition was that the highly structure-sensitive anisotropy is caused by the variable degree of faulting. For fields parallel to the *c*-axis, the faulted planes (or regions) might constitute barriers, impeding the flow of current but increasing the probability of excitation by those electrons which do penetrate them. Under strong photoconductive excitation, the effects of

the barriers would be diminished and a less pronounced anisotropy would be expected.

In accordance with these ideas, the precession diagrams for the crystals of Table I were examined, and the crystals are listed in this table in order of increasing density of streaking relative to the density of prominent spots. This can be, at best, only a rough measure of the stacking disorder, since various size and shape factors enter into the relative intensities, and since the effects of polytypes (stacking disorder) is difficult to assess. Nevertheless, there is a trend towards an increase in the dark current and photocurrent anisotropies as we proceed down Table I. The lack of correlation in light output shows, however, that other factors such as, perhaps, the distribution of impurities, also play important roles. It is hoped that the preparation of more nearly perfect crystals, together with a quantitative evaluation of their disorder, will shed more light on this problem.

Thanks are due Dr. J. L. Birman for several discussions and Dr. G. Neumark, Dr. H. Samelson, W. S. Romito, and S. R. Kellner for assistance in the measurements.

⁵L. W. Strock and V. A. Brophy, *Am. Mineralogist* **40**, 94 (1955).

⁶Short, Steward, and Tomlinson, *Nature* **177**, 240 (1956).

Theory of the Forbidden Transitions of Nitrogen Atoms Trapped in Solids*

C. M. HERZFELD

National Bureau of Standards, Washington, D. C., and Department of Physics, University of Maryland, College Park, Maryland

(Received May 29, 1957)

A detailed theory of the forbidden transitions of nitrogen atoms trapped in solids is given. The trapped atoms are perturbed by the solid. Configuration interaction, produced by the solid, is important. Splittings and shifts of levels, and reduction of half-lives are explained in one consistent scheme. The trapping sites of atoms are shown to have low symmetry and to be nearly identical for different atoms.

1. INTRODUCTION

IN a recent paper¹ a qualitative theory for some of the spectroscopic observations by Broida and co-workers² on trapped nitrogen atoms was given. In their experiments nitrogen gas was passed at about one millimeter pressure through a 2450-Mc electric discharge and the discharge products frozen on a surface kept at 4.2°K. A series of glows and flashes were observed, whose spectra indicated the presence of nitrogen atoms in the deposit, trapped along with nitrogen molecules. Many features of the spectra were interpreted successfully.

1. It was assumed that some of the trapped nitrogen atoms were deposited while in the excited state $2p^3\ ^2D$, and went by a radiative process to the ground state $2p^3\ ^4S$. The neighboring molecules were assumed to perturb this transition.

2. It was further assumed that recombination of atoms produced excited N_2 molecules in the state $^5\Sigma$, which went by a radiative transition to the state $^3\Sigma$.

The present paper reports a detailed examination of the perturbing effects of neighboring molecules on the transition $2p^3\ ^2D \rightarrow 2p^3\ ^4S$, and the resulting theory makes it possible to explain completely the relevant experimental results. It may be well to summarize the experimental data² first. Table I shows the position and relative intensities of plate blackenings of the spectral lines emitted by the solid which are to be associated with the $^2D \rightarrow ^4S$ transition. The positions of these lines, which we call "α lines," are accurately known, and they

* This research was supported by the U. S. Air Force through the Air Force Office of Scientific Research of the Air Research and Development Command.

¹C. M. Herzfeld and H. P. Broida, *Phys. Rev.* **101**, 606 (1956).

²A. M. Bass and H. P. Broida, *Phys. Rev.* **101**, 1740 (1956); H. P. Broida and J. R. Pellam, *Phys. Rev.* **95**, 845 (1954).

TABLE I. Some intense lines emitted from the condensed solid nitrogen.

λ , Å (air)	ν , cm ⁻¹ (vacuum)	Rel. intens. <i>I</i>
5214.2	19173.1	2
5220.1	19151.4	8
5228.5	19120.6	10
5235.0	19096.9	6
5240.4	19077.2	4

are quite sharp with half-widths of about one cm⁻¹. The half-life of the strongest line has been measured to be approximately 10 to 20 seconds. The corresponding transitions of the free N atom, $2p^3\ ^2D_{3/2}$ and $2p^3\ ^2D_{3/2} \rightarrow 2p^3\ ^4S_{3/2}$, occur at 19 223 and 19 231 cm⁻¹, respectively.³ The half-life of these highly forbidden transitions is known to be about 20 hours.⁴

If the α lines arise from these forbidden transitions three effects must be explained:

1. The two lines of the free-atom transition are split into five lines for the trapped atom, with the separations given in Table I.
2. The center of gravity of the free-atom lines is shifted by 102 cm⁻¹ to the red in the trapped atom.
3. The half-life is reduced from 20 hours to about 15 seconds.

These three effects can be explained in detail by calculating the perturbing effect of neighboring molecules on the trapped atoms. The perturbations are assumed to arise from the electric quadrupole moments of the N₂ molecules which surround the atoms and their effect can be calculated with crystal field theory.⁵ The Hamiltonian for a trapped N atom can be written schematically in the form

$$H = F(i) + G(i, j) + E(\mathbf{s}_i, \mathbf{l}_i) + V, \quad (1)$$

where $F(i)$ consists of the kinetic energy, and the potential energy in the field of the nucleus, of the electrons of the N atom. $G(i, j)$ is the electrostatic repulsion energy of these electrons. The terms $F(i)$ and $G(i, j)$ are assumed to be diagonalized, and the calculation begins in the *SLJM* representation. The term $E(\mathbf{s}_i, \mathbf{l}_i)$ consists of the spin-orbit, spin-spin, and spin-other-orbit interactions of the electrons of the N atom and accounts for the split in the 2D term of the free atom.^{4,6} V describes the perturbation of the electrons of the N atom by the neighboring molecules. It depends on the arrangements of these neighbors and must account for the three differences between the free and trapped atoms.

The present theory consists of finding a V which will

³ *Atomic Energy Levels*, U. S. National Bureau of Standards Circular No. 467 (U. S. Government Printing Office, Washington, D. C., 1948), Vol. 1.

⁴ C. W. Ufford and R. M. Gilmore, *Astrophys. J.* **111**, 580 (1950).

⁵ B. Bleaney and K. W. H. Stevens, *Reports on Progress in Physics* (The Physical Society, London, 1953), Vol. 16, p. 108.

⁶ Aller, Ufford, and Van Vleck, *Astrophys. J.* **109**, 42 (1949).

give a trapped-atom spectrum in agreement with experiment, and then interpreting this V in terms of a geometrical model of atoms and molecules.

The formal part of the theory is straightforward and the results are quite definite and reliable. A general V can be written down which depends primarily on the symmetry of the problem, and which contains the magnitudes of the interactions as unknown parameters. The predictions of the theory are then fitted to the data by adjusting the values of the parameters. Thus, the separations of the α lines, their shift from the free-atom transition, and their relative intensities can be explained in one consistent scheme.

In the second part numerical estimates of the parameters are made, using a detailed model. Such calculations, if made rigorously, would be equivalent to the solution of a molecular orbital problem for a many-atom, many-center system, and therefore quite difficult. Careful approximate methods are sometime successful,^{7,8} but involve lengthy computation. The present study limits itself to relatively crude numerical estimates of the parameters for various geometrical models. Estimates for a few of these models give adequate agreement with the values obtained by fitting the data. Thus, the over-all reasonableness of the theory is verified, and the range of possible molecular models is greatly restricted.

The states whose perturbations are of primary interest in this theory are $2p^3\ ^2D$ and $2p^3\ ^4S$. General considerations as well as direct calculations show that all matrix elements of V of the type $\langle 2p^3\ SLM_S M_L | V | 2p^3\ SLM_S M_L' \rangle$ vanish identically, because the p shell is half-filled. Therefore the observed changes in the spectrum on trapping the atoms must be caused by interactions between the levels $2p^3\ ^2D$ and $2p^3\ ^2P$, and by configuration interaction. Configuration interaction is very difficult to treat completely with rigor, and we do not attempt this here. Rather we investigate the effect of the $2p^3\ ^2P$ level in detail, and also that of the lowest levels of the lowest configurations which can play a role in this mechanism. This procedure is incomplete but affords the possibility of doing a relatively simple calculation completely. The configurations which provide the basis for the calculation are $2p^3$, $2p^2\ 3s$, and $2p^2\ 3p$.

2. FORMAL THEORY

A. General Considerations

The perturbation energy of an N atom by its neighbors can be expanded in a Taylor's series in the coordinates of the electrons of the atom, about the nucleus of the atom. The perturbing potential energy is then of the form

$$V = V_0 + V_1 + V_2 + \dots, \quad (2)$$

⁷ W. H. Kleiner, *J. Chem. Phys.* **20**, 1784 (1952).

⁸ Y. Tanabe and S. Sugano, *J. Phys. Soc. Japan* **9**, 753, 766 (1954); **11**, 864 (1956).

where V_0 is a constant, V_1 a linear function of the electron coordinates, V_2 a quadratic function, etc. Because we consider the effect of V on s and p electrons only, all matrix elements of $V_{k>2}$ vanish rigorously. The detailed form of the terms V_k depends on the geometrical details of the model. We present first the theory for a model with a symmetry which gives agreement with experiment, and consider later those alternatives which can be ruled out.

This model is of the following general type: the N atom is assumed to lie closer to one neighboring molecule than to the others, so that the symmetry of the perturbation as well as the major contributions to its magnitude are determined by one molecule. Figure 1 shows the arrangement and defines the coordinate system. The potential in this system has cross-terms of the form $(y-y_0)(z-z_0)$. A rotation in the y - z plane, depending on d and θ , can be found which suppresses this cross-term. In the new coordinate system

$$V = V_0 + \alpha u + \beta w + \gamma u^2 + \delta v^2 - (\gamma + \delta)w^2. \quad (3)$$

The constants α , β , etc., are functions of d , θ , and the electric quadrupole moment of the molecule. The variables u , v , and w are linear functions of $(x-x_0)$, $(y-y_0)$, and $(z-z_0)$. The potential satisfies Laplace's equation.

The theory involves the calculation of the quantum-mechanical averages of the effects of V on the states $2p^3\ ^2P$, $2p^3\ ^2D$, and $2p^3\ ^4S$, taking configuration interaction with $2p^2\ 3s$ and $2p^2\ 3p$ into account.

B. The Splitting and the Shift

The constant term V_0 plays no role because it affects all levels equally. The linear term V_1 increases the transition probability for the $^2D \rightarrow ^4S$ transition. The quadratic term V_2 produces the splitting of the levels, and much of their shifts, and we investigate its effects in this section. Figure 2 indicates these effects schematically.

The most important contribution to the splitting comes from the matrix elements of form

$$\langle 2p^3\ ^2DJM | V_2 | 2p^3\ ^2PJ'M' \rangle.$$

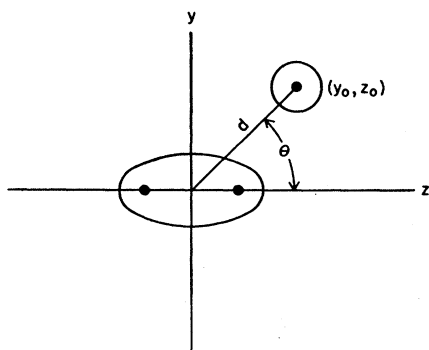
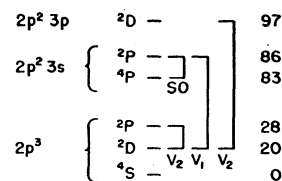


FIG. 1. The model for an N atom trapped near an N_2 molecule.

Fig. 2. Schematic summary of levels involved in the calculation. SO represents mixing through spin-orbit coupling, V_1 through linear potential terms, V_2 through quadratic potential terms. Numbers on the right give energy in units of 1000 cm^{-1} .



Additional contributions will be made by the levels such as $2p^2(^3P)3p\ ^2D$, which lies about $8 \times 10^4\text{ cm}^{-1}$ above the $2p^3\ ^2D$ level.³ These effects explain completely the observed splittings, and much of the observed shift. The calculation must take into account the magnetic interactions $E(\mathbf{s}_i, \mathbf{l}_i)$ for the $2p^3\ ^2D$ level^{4,6}:

1. The second-order spin-orbit coupling $E(\mathbf{s}_i \cdot \mathbf{l}_i)$ mixes the 2D and 2P levels of $2p^3$ and contributes of the order of one cm^{-1} to the splitting of the 2D in the free atom. It cannot be disregarded here because these matrix elements mix with the crystal field elements in the perturbation calculation. The matrix elements are given in Condon and Shortley.⁹

2. The spin-spin coupling $E(\mathbf{s}_i \cdot \mathbf{s}_j)$ mixes the 2D and 4S levels of $2p^3$. This effect contributes about one cm^{-1} to the splitting and is neglected in our calculation. The transition probability for $^2D \rightarrow ^4S$ of the free atom is affected strongly by this, but the effect is too small to matter for the transitions of the trapped atom.

3. The spin-other-orbit coupling $E(\mathbf{s}_i \cdot \mathbf{l}_j)$ must also be taken into account. The relevant matrix elements are given by Aller, Ufford, and Van Vleck⁶:

$$\begin{aligned} \langle ^2D_{\frac{3}{2}} | E | ^2D_{\frac{3}{2}} \rangle &= -(37/5)\eta, \\ \langle ^2D_{\frac{5}{2}} | E | ^2D_{\frac{5}{2}} \rangle &= (111/10)\eta, \end{aligned} \quad (4)$$

where η is an integral over the wave functions of the $2p$ electrons which gives the magnitude of the interaction. The value of η for the free atom can be determined by direct calculation or by fitting the theoretical splittings of the 2D and 2P levels to the observed splittings of the free atom. Fitting the most recently observed splittings gives $\eta = 0.715\text{ cm}^{-1}$ for the free atom.¹⁰

The matrix elements of type $\langle 2p^3\ ^2D | V_2 | 2p^3\ ^2P \rangle$ are calculated by using angular parts of wave functions obtained by standard methods (TAS, Chap. 8). The term V_2 of Eq. (3) can be written as a linear combination of spherical harmonics of degree 2, multiplied by $r^2 = u^2 + v^2 + w^2$. The matrix elements are then linear combinations of terms having three factors each. The first factor (r^2) is a radial integral of r^2 times two $2p$ radial one-electron wave functions. The second factor is an integral of a product of three associated Legendre polynomials of second degree, is proportional to a specific Wigner coefficient, and can be obtained directly from the tables in TAS, Chap. 6. The third factor is an integral of products of the form $\exp(im\phi)$ and is evaluated directly. V_2 has

⁹ E. U. Condon and G. H. Shortley, *The Theory of Atomic Spectra* (Cambridge University Press, New York, 1951), second edition, Chap. 11. Hereafter referred to as TAS.

¹⁰ I. S. Bowen, *Astrophys J.* **121**, 306 (1955).

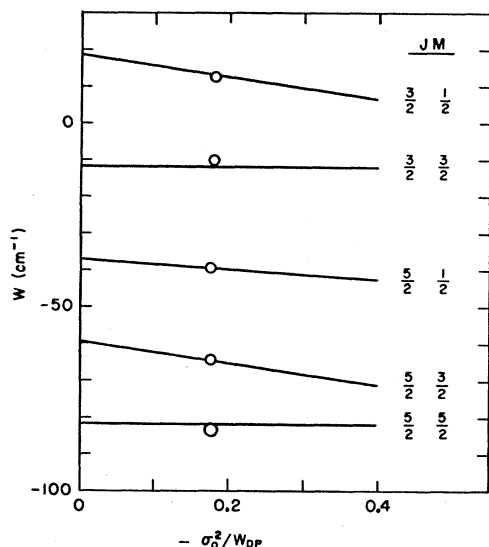


FIG. 3. Comparison of theoretical eigenvalues of $V_2 + E(s_i, l_i)$ with experimental levels. Theoretical eigenvalues are plotted versus $-\sigma_0^2/W_0P$, for $|\sigma_2| = 230 \text{ cm}^{-1}$, and $\eta = 3.46 \text{ cm}^{-1}$. Circles indicate experimental values; diameters of circles indicate experimental uncertainties.

no elements of type $\langle 2p^3 \ ^2D | V_2 | 2p^3 \ ^2D \rangle$, and hence the eigenvalues of V_2 can be obtained by second-order perturbation theory. They are:

$$\begin{aligned}
 W(^2D \ ^{5/2} \pm \ ^{5/2}) &= W_0 - \frac{37}{5} \eta + \frac{8\sigma_2^2}{W}, \\
 W(^2D \ ^{5/2} \pm \ ^{3/2}) &= W_0 - \frac{37}{5} \eta + \frac{144\sigma_0^2}{5W} + \frac{24\sigma_2^2}{5W}, \\
 W(^2D \ ^{5/2} \pm \ ^{1/2}) &= W_0 - \frac{37}{5} \eta + \frac{72\sigma_0^2}{5W} + \frac{8\sigma_2^2}{5W}, \\
 W(^2D \ ^{3/2} \pm \ ^{3/2}) &= W_0 + \frac{111}{10} \eta + \frac{36\sigma_0^2}{5W} + \frac{36\sigma_2^2}{5W} + \frac{5\zeta^2}{4W} + \frac{6\sigma_0\zeta}{W}, \\
 W(^2D \ ^{3/2} \pm \ ^{1/2}) &= W_0 + \frac{111}{10} \eta + \frac{108\sigma_0^2}{5W} + \frac{12\sigma_2^2}{5W} + \frac{5\zeta^2}{4W} + \frac{6\sigma_0\zeta}{W}.
 \end{aligned} \tag{5}$$

Here W_0 is the unperturbed energy of the level $2p^3 \ ^2D$, $W = W(2p^3 \ ^2D) - W(2p^3 \ ^2P) = -7600 \text{ cm}^{-1}$, $\zeta = 90 \text{ cm}^{-1}$ is the spin-orbit coupling constant for the $2p^3$ configuration,⁴ η the spin-other-orbit coupling constant, and σ_0 and σ_2 are two crystal field splitting constants. The perturbation leaves M_L an approximately good quantum number, and σ_2 enters only as the square.

We have not shown here the effects of the level $2p^2 \ 3p \ ^2D$. These are smaller by a factor of twenty than those considered here, and do not change the result for the splittings significantly. It is possible to show that the effect of V_2 on $2p^3 \ ^4S$ is small, much less than one

cm^{-1} . Therefore the observed splittings and shifts of the α lines must be attributed to changes in the level $2p^3 \ ^2D$ and should therefore be given by the Eqs. (5). The eigenvalues of Eqs. (5) contain two undetermined parameters: σ_0 , σ_2 , and two atomic parameters, ζ and η . The values of ζ and η are known for the free atom, but steadily accumulating evidence shows that all atomic integrals (such as Slater integrals, spin-orbit coupling constants, etc.) are modified in a solid. We have decided, more or less arbitrarily, to allow adjustments in η , but to leave ζ fixed. The constants σ_0 and σ_2 are unknown. Numerical estimates of them are given in Sec. 3. The three parameters σ_0 , σ_2 , and η are adjusted to give agreement between the observed levels and the predicted ones. There are four observed energy differences between the α lines, hence any agreement so obtained is not trivial.

Figure 3 shows the eigenvalues for $|\sigma_2| = 230 \text{ cm}^{-1}$ and $\eta = 3.46 \text{ cm}^{-1}$ as a function of σ_0 , together with the levels inferred from the data in Table I.

The agreement between the predicted and the observed relative separations of the levels is seen to be very good. A slight improvement of the fit might be obtained by revising the values of the parameters, but this would be pointless, because experimental uncertainties and the neglected configuration interaction and spin effects are of the same magnitude as the possible improvements. Fitting the eigenvalues of this three-parameter problem to the data was a lengthy procedure, and in particular, the relatively large value of η necessary to obtain agreement was unexpected. Only after considerable searching for combinations with smaller η proved unsuccessful was the present value adopted. Variation of ζ , leaving η fixed, does not give agreement with experiment.

The choice of parameters which gives agreement between the predicted and observed separation of levels also predicts a lowering (with respect to the ground state) of the center of gravity of the 2D levels by 37 cm^{-1} . The observed lowering is 102 cm^{-1} . Thus the same choice of parameters which gives complete agreement for the relative positions also predicts about one-third of the observed shift in the lines. Configuration interaction with $2p^2 \ 3p \ ^2D$ contributes an additional splitting equal to about 3% of the total and has been neglected in our calculation. It also contributes about 5% to the shift, thus relatively much more to the shift than to the splitting. It is thus qualitatively clear that all possible configuration interactions can account for the rest of the shift. Agreement is obtained only for negative σ_0 , which limits the possible geometry of the atom sites. The Eqs. (5) were derived assuming $\gamma \neq \delta$ in Eq. (3). If the atom is in a site having a C_∞ axis, then $\gamma = \delta$ and $\sigma_2 = 0$. In this case the eigenvalues cannot be fitted to the observed levels, because they fall into two widely separated groups of closely spaced levels. A discussion of the interpretation of the values of the parameters and what they imply about the atom sites will be given in Sec. 3.

C. Transition Probabilities

The formal model which correctly predicts the positions of the spectral lines also correctly predicts their relative intensities. Configuration interaction is assumed to determine the transition probabilities. We discuss here only such mixing of states which favors electric dipole transitions. The perturbation V will also increase the probability for electric quadrupole and magnetic dipole transitions, but this effect is negligible compared to the increase in the electric dipole transition probability.

The levels whose admixture to $2p^3\ ^2D$ is important are $2p^2\ 3s\ ^2P$ and $2p^2\ 3s\ ^4P$. The 2P and 4P levels are mixed by spin-orbit coupling to the extent that Russell-Saunders coupling is broken down. (See Fig. 2.) The 2P state is mixed into the $2p^3\ ^2D$ state by the perturbation V_1 . The over-all effect is to introduce into the $2p^3\ ^2D$ a small amount of $2p^2\ 3s\ ^4P$. Because the transition $2p^2\ 3s\ ^4P \rightarrow 2p^3\ ^4S$ is completely allowed, the small admixture of 4P with 2D has a striking effect on the transition probabilities.

The calculations of the transition probabilities are lengthy and only an outline is given here. The mixing of $2p^2\ 3s\ ^2P$ and $2p^2\ 3s\ ^4P$ is calculated from the formulas of TAS (Chap. 11), using the observed separation of 2P and 4P and the spin-orbit coupling constant for the free atom. The matrix elements for V_1 which connect the $2p^3\ ^2D$ states with the $2p^2\ 3s\ ^2P$ states are easily calculated by methods analogous to those discussed for V_2 above.

The admixture of 4P and 2P levels to the $2p^3\ ^2D$ level is then obtained by perturbation theory. The atomic states in the solid are finally presented in the form

$$|^2DJM\rangle = |2p^3\ ^2DJM\rangle^0 + \sum_i a_i |2p^2\ ^2PJ'M'\rangle + \sum_k b_k |2p^2\ 3s\ ^2Pk\rangle + \sum_l c_l |2p^2\ 3s\ ^4Pl\rangle. \quad (6)$$

It should be noted that the $|^2DJM\rangle$ are mixtures of states with opposite parity. This mixing is the result of V_1 (which has odd parity) and is the basic reason for the larger transition probability for the trapped atom.

The lower state of the transition under study is $2p^3\ ^4S$. Theoretical considerations as well as experimental evidence indicate that this state is almost completely unperturbed. The matrix elements which give the transition probability are, therefore, proportional to $|\langle ^4S\bar{M}_S | \mathbf{P} | ^2DJM \rangle|^2$, where \mathbf{P} is the electric dipole vector, and \bar{M}_S indicates that the ground state is a linear combination with average M equal to zero.

The Einstein transition probabilities for the five lines are obtained by direct computation. The results are

$$\begin{aligned} A(\frac{5}{2} \pm \frac{5}{2}) &= A_0 1.540 K_1^2, \\ A(\frac{5}{2} \pm \frac{3}{2}) &= A_0 \{0.618 K_0^2 + 1.222 K_1^2\}, \\ A(\frac{5}{2} \pm \frac{1}{2}) &= A_0 \{1.222 K_0^2 + 0.618 K_1^2\}, \\ A(\frac{3}{2} \pm \frac{3}{2}) &= A_0 \{0.154 K_0^2 + 0.571 K_1^2\}, \\ A(\frac{3}{2} \pm \frac{1}{2}) &= A_0 \{0.220 K_0^2 + 0.043 K_1^2\}. \end{aligned} \quad (7)$$

TABLE II. Relative transition probabilities.

Line	Observed	Calculated
$\frac{5}{2} \pm \frac{5}{2}$	2	1
$\frac{5}{2} \pm \frac{3}{2}$	8	3
$\frac{5}{2} \pm \frac{1}{2}$	10	10
$\frac{3}{2} \pm \frac{3}{2}$	6	8
$\frac{3}{2} \pm \frac{1}{2}$	4	5

In these equations $A_0 = TS^2\rho^2 |\langle ^4S | \mathbf{P} | ^4P \rangle|^2$, where T is a collection of fundamental and numerical constants,

$$S = \frac{\langle 2p | r | 3s \rangle}{W(2p^3\ ^2D) - W(2p^2\ 3s\ ^2P)},$$

$$\rho = \frac{\zeta_p}{W(2p^2\ 3s\ ^4P) - W(2p^3\ ^2D)},$$

where ζ_p is the one-electron integral for the spin-orbit coupling, and

$$K_0 = 2\beta e_0 (\pi/3)^{\frac{1}{2}},$$

$$|K_1| = 2\alpha e_0 (2\pi/3)^{\frac{1}{2}},$$

where α and β are given in Eq. (3) and e_0 is the electronic charge. The observed plate-blackening of Table I are proportional to the logarithms of the intensities of the lines, and hence approximately proportional to the transition probabilities. It is possible to calculate the relative transition probabilities from Eq. (7) as a function of K_0^2/K_1^2 , if we assume that the excited levels are initially equally populated, and to compare the calculated transition probabilities with the observed ones. If $K_0^2/K_1^2 = 2$, good agreement with experiment is found; the resulting relative transition probabilities are shown in Table II. The observed relative transition probabilities are uncertain by about 30%, and the predicted ratios fall more or less within this limit of error.

The terms in the Eqs. (7) proportional to K_1^2 arise from a term in V_1 proportional to $P_1^1(\cos\theta)$. This term is necessary to get comparable transition probabilities for all five transitions. Without it, line $(\frac{5}{2} \pm \frac{5}{2})$ would have zero probability for electric dipole transitions (at least in the present approximation) and would hardly be observable, and the relative transition probabilities for the other four lines would be quite different than the observed ones.

3. MODELS AND NUMERICAL ESTIMATES

A. Symmetry of the Model

The form of the potential of Eq. (3) allows us to rule out a number of models completely. The potential must contain terms proportional to $P_1^1(\cos\theta)$ and $P_2^2(\cos\theta)$ for the theory to agree with experiment. This eliminates completely the possibility of atomic sites with two fold and higher axes of symmetry. For example, a substitution of an atom for a molecule in the low-temperature

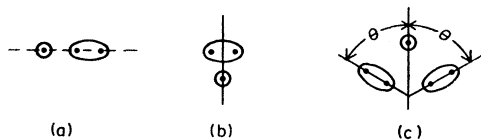


FIG. 4. Examples of trapping sites which are ruled out by theory. Three-dimensional sites with C_2 or axes of higher symmetry are also ruled out.

form of solid N_2 , without appreciable rearrangement, would leave the atom in a site with C_{3v} symmetry. This would require the vanishing of P_1^1 and P_2^2 terms in V . Other models which are excluded by such arguments are shown in Fig. 4.

The model with correct symmetry is that shown in Fig. 1, with $0 < \theta < \pi/2$. It may be well to emphasize again that the potential arising from the quadrupole moment of the N_2 molecule falls off very rapidly with distance. Thus, if the N atom is somewhat closer to one molecule than to the others, this nearest molecule will make the greatest contribution to V , and the relative geometrical configuration of this molecule and the atom will decide the symmetry and the major contributions to V .

B. Numerical Estimates

The crystal field parameters occurring in the theory are estimated from a classical point-charge model of the N_2 molecule. This procedure is not very reliable, but gives some insight if the results are not taken too seriously.

The electric quadrupole moment Q of the N_2 molecule in the gas is known from pressure broadening of microwave spectra to be $Q = 0.27e_0 \times 10^{-16}$ cm², with e_0 in electrostatic units.¹¹ The value for molecules in the solid is not known, but the approach is so crude that the difference is not important. A point-charge model with positive charges equal to $\frac{1}{4}e_0$ at the two nuclei of the N_2 molecule, and a negative charge $\frac{1}{2}e_0$ between the nuclei, has almost exactly the required quadrupole moment. The higher moments of the molecule are represented poorly by this model, but involve terms $V_{k>2}$, which do not contribute to the matrix elements in our approximation.

The classical potential energy V can be expanded explicitly for the point-charge model with the geometry shown in Fig. 1, and transformed to the form in Eq. (3). Each coefficient in Eq. (3) is then given in terms of the geometrical constants and the charge distribution of the model. These relations are complicated and not sufficiently general to warrant their publication here. It is easy to calculate σ_0 and σ_2 in terms of these coefficients, and to estimate σ_0 and σ_2 numerically for different distances and orientations. All necessary expressions are readily calculated, and the relevant atomic integrals

¹¹ C. Greenhow and W. V. Smith, J. Chem. Phys. **19**, 1298 (1951).

can be estimated roughly using Slater wave functions for N atoms. Similarly the transition probability parameters α and β are readily evaluated, and A_0 estimated. It is found that several geometrical arrangements give reasonable results, but the best compromise model has $d = 2.5$ Å and $\theta = 0.86$ radians (50 degrees). The significant numerical constants for this model are shown in Table III. The agreement is reasonably good. The predicted crystal field splitting constants are of the right order of magnitude, while the predicted transition probabilities are somewhat too small. The calculation of the transition probabilities requires a value for A for the allowed transition $2p^2 3s^4 P \rightarrow 2p^3 4S$. This is apparently not known, and has been assumed to be 10^{-7} sec⁻¹. An estimate of $\langle 2p | r | 3s \rangle$ was obtained by using hydrogen atom functions.

On the whole the direct numerical estimates give results no worse than is usual in such an approach. We can give here no explanation for the change of the spin-orbit coupling constant from 0.715 cm⁻¹ in the gas to 3.46 cm⁻¹ in the solid. In fact a change in η by a factor of 5 implies large changes in the Slater integral F_2 , and hence changes in the separation of the 2D and 4S levels larger than are observed.¹² It is thus likely that an unknown physical effect contributes to these matrix elements.

The width of the observed lines and the spread in measured half-lives make possible an estimate of the variations in the sites of different N atoms. This can be done by assuming that the theory gives correctly the dependence of the parameters on geometry even though it does not give their absolute values correctly. The α lines are quite sharp, one cm⁻¹ or less. This implies that all radiating N atoms are located in substantially the same environment. Calculation shows that a spread in the distances d for different atoms of approximately 0.1 Å and a spread of one degree in the angle θ would change the levels by about the line width. Similarly variations in d by 0.1 Å and in θ by two degrees imply a spread in the half-life of a factor of two. Thus it is seen that all the excited N atoms must be in almost exactly the same types of sites to produce such narrow lines with such definite half-lives. The implications of this are discussed below.

4. DISCUSSION

The calculations reported here confirm the presence of nitrogen atoms in the low-temperature deposits from

TABLE III. Comparison of predicted and observed parameters.

	Best model	Observed
σ_0	-85 cm ⁻¹	-37 cm ⁻¹
σ_2	110 cm ⁻¹	± 220 cm ⁻¹
K_0^2/K_1^2	2.0	2.0
$A(\frac{3}{2}, \frac{3}{2})$	0.02 sec ⁻¹	0.05 sec ⁻¹

¹² R. E. Trees (private communication).

electric discharges. The formal crystal field theory gives excellent agreement with experiment when a small number of parameters are suitably adjusted. The agreement of the formal theory shows it to be a powerful tool for the study of systems from the first row of the periodic table of elements. Crude numerical estimates of the parameters agree as well as can be expected with the values obtained from the data using the formal theory.

The symmetry of the sites of excited atoms has been shown to be very low, but the sites of different excited atoms are seen to be identical, or nearly so. It is not yet clear how best to explain this. We believe at present that each excited N atom is linked in a loose molecular complex to a particular N₂ molecule. The link must be quite weak to modify the spectrum so slightly from that of a free atom. Were this link as strong as an ordinary nitrogen-nitrogen single bond, the observed spectrum would bear no resemblance to that of the free N atom. Thus, it is very unlikely that the systems discussed in this paper are the N₃ molecules proposed by Pimentel and his collaborators.¹³ This implies no conflict of interpretations, since the two different interpretations are based on quite different sets of observations. The present theory allows no direct deductions about the sites of the atoms after they radiate. It is possible that they move to a quite different position after the transition. The α lines have sharp edges toward the violet, and diffuse edges toward the red. This can be interpreted to mean that the atoms acquire translation kinetic energy during transition to the ground state. The presence of N atoms in deposits of the kind considered has recently been verified by Jen,¹⁴ who has found in these systems paramagnetic resonance absorption by very slightly perturbed N atoms in the ground state.

In the earlier interpretation¹ a tentative explanation of the β lines (a group of three broad lines near 5600 Å) was given. This explanation is now seen to be untenable, because direct crystal field effects for the highly excited states which were then postulated should be several orders of magnitude greater than the splittings of the β lines. It is possible that the β lines correspond to a transition of the type $2p^3\ ^2D \rightarrow 2p^3\ ^4S$ in which the excited atom is in a different site than that which produces the α lines. If d is much less than 2.5 Å, say

¹³ Milligan, Brown, and Pimentel, *J. Chem. Phys.* **25**, 1080 (1956).

¹⁴ C. K. Jen (private communication).

1.5 to 2.0 Å, and $\theta=0$ or $\pi/2$, then four broad lines may be expected, which may appear as three lines. The half-life would be expected to be much shorter than that of the α lines, in agreement with experiment. The observed over-all spread of 300 cm⁻¹, red-shift of 1000 cm⁻¹, and half-life less than 0.1 sec are quite compatible for such a model. Again the red edges of the lines are much more diffuse than the violet edges, suggesting that a bound excited state goes to a ground state where the atom has some kinetic energy of translation.

An explanation can now be given of the weak long-lifetime emission line at 5940 Å, suggested by a remark of Vegard. The line at 5940 Å lies 2290 cm⁻¹ to the red of the strongest of the α lines. The energy of vibrational excitation of an N₂ molecule in its ground state is 2330 cm⁻¹ when the molecule is in the gas or in the liquid. The value for the solid is not yet known. Two possible explanations of the 5940 Å line suggest themselves: Either some quanta of the α emissions get Raman-scattered on their way through the solid by N₂ molecules or the emissions of the α quanta leave some N₂ molecules of the "molecular complexes" in an excited vibrational state. One of these alternatives can be ruled out when the Raman spectrum of solid N₂ is better known, because only if the vibrational Raman frequency of ordinary N₂ molecules in the solid is 2290 cm⁻¹ is the first alternative correct. In either case all five α lines should be found repeated with low intensity near 5940 Å. The one line so far observed corresponds probably to the strongest α line. More intensive search may lead to the others.

5. ACKNOWLEDGMENTS

The search for the values of the parameters which give agreement with experiment was long and tedious, and D. Levine of NBS completed it successfully. H. Goldberg of NBS carried out the computations of the electrostatic field about the N₂ molecule. Dr. Charlotte Moore Sitterly of NBS contributed greatly by her interest in this problem, and supplied the author with the latest news about the spectrum of atomic nitrogen, and Dr. R. E. Trees of NBS made valuable comments about the general approach. The lively discussions with Dr. C. K. Jen of the Applied Physics Laboratory of the Johns Hopkins University, Dr. G. Pimentel of the University of California, and with the author's colleagues at NBS have served to clarify many questions.